

Original Article

Interaction of phenotypic sublines isolated from triple-negative breast cancer cell line MDA-MB-231 modulates their sensitivity to paclitaxel and doxorubicin in 2D and 3D assays

Indrė Januškevičienė, Vilma Petrikaitė

Laboratory of Drug Targets Histopathology, Institute of Cardiology, Lithuanian University of Health Sciences, Sukilėlių pr., LT-50162, Kaunas, Lithuania

Received May 5, 2023; Accepted June 23, 2023; Epub August 15, 2023; Published August 30, 2023

Abstract: Breast cancer is a rapidly evolving, multifactorial disease that accumulates numerous genetic and epigenetic alterations. These result in molecular and phenotypic heterogeneity within the tumor, the complexity of which is further amplified through specific interactions between cancer cells. We aimed to analyze cell phenotypic sublines and the influence of their interaction on drug resistance, spheroid formation, and migration. Seven sublines were derived from the MDA-MB-231 breast cancer cell line using a multiple-cell suspension dilution. The growth rate, CD133 receptor expression, migration ability, and chemosensitivity of these sublines to anticancer drugs doxorubicin (DOX) and paclitaxel (PTX) were determined. Three sublines (F5, D8, H2) have been chosen to study their interaction in 2D and 3D assays. In the 2D model, the resistance of all sublines composition to DOX decreased, but in the 3D model, the resistance of all sublines except H2, increased to both PTX and DOX. In the 3D model, the combined sublines F5 and D8 had higher resistance to DOX and statistically significantly lower resistance for PTX compared to the control. The interaction between cancer stem-like cells (F5) and increased migration cells (D8) increased resistance to PTX in cell monolayer and increased resistance against both DOX and PTX in the spheroids. The interaction of DOX-resistant (H2) cells with other cell subpopulations (D8, F5, HF) decreased the resistance to DOX in cell monolayer and both DOX and PTX in spheroids.

Keywords: Triple-negative breast cancer, cell interaction, drug resistance, phenotypic sublines, MDA-MB-231

Introduction

Breast cancer is one of the most common oncology diseases worldwide. In 2020, the predicted number of new breast cancer cases was 2.3 million and 685,000 deaths globally (based on World Health Organization (WHO) data) [1]. Over the past few decades, significant progress has been made in preventing, diagnosing, and treating cancer. TNBC accounts for about 15-20% of all biological types of breast cancer [2]. Based on the histological classification of breast tumors, TNBC is classified as invasive ductal, less commonly metaplastic, medullary, or adenoid cystic carcinoma. Invasive ductal carcinoma is the most common (70-80%) form of breast cancer [3]. These tumors begin to develop in the milk ducts from the epi-

thelial cells that line them. Based on molecular profiling studies, since 2011, many TNBC subtypes have been established [4]. Still, there is no one unique official classification due to the TNBC cell variability [5-8]. Burstein et al. divided TNBC into four stable, distinct molecular subtypes that differentially respond to chemotherapy and targeted-therapy agents: basal-like immune-suppressed subtype, basal-like immune-activated subtype, mesenchymal subtype, luminal androgen receptor subtype. This new classification was suggested by combined early years studies [9].

Each molecular subtype has a different response to the treatment [4, 9]. Molecular profiling studies indicate that most TNBCs (approximately 70%) tumors consist of basal subtype

Interaction of phenotypic sublines isolated from MDA-MB-231 cell line

cells. The rest of these tumors consist of various molecular subtypes of TNBC cells that are biologically distinct. This intratumor cell heterogeneity usually is responsible for the failure of treatment of disease due to the drug-resistant cell populations in tumors. These drug-resistant cell populations lead the tumor relapse and cancer progression. Intratumor cell heterogeneity is believed to form differently and can be detected at the morphological and molecular heterogeneity [10]. Morphological heterogeneity is observed as tumor histology (histotype, tissue reaction, differentiation, tissue composition) and different functional areas (tumor center and borders). These differences could cause clinical misinterpretation of the future tumor treatment strategy [11]. Molecular intratumor heterogeneity is divided into two types: first is clonal heterogeneity (genetic or epigenetic evolution) and nonclonal heterogeneity (phenotypic functional plasticity or stochastic (single cell plasticity) [12].

TNBC tumor heterogeneity makes the treatment of these tumors very complicated. The treatment options for this disease are limited because the cells do not have targets on which to tailor the treatment. Patients whose tumors are in later stages have a very poor survival prognosis. TNBC positively responds to chemotherapy (anthracyclines or/and taxanes-based) [13]. However, more than 50% of patients diagnosed with TNBC at an early stage have a recurrence of the disease, and 37% of these patients die within the first five years, despite the treatment being applied [14]. Many drug resistance mechanisms are described, such as impaired drug influx, enhanced drug efflux via multidrug resistance pumps, drug compartmentalization away from its target protein, metabolic drug inactivation and drug resistance due to cancer cell-cell and cancer cell-stromal cell interaction [15]. Cell interaction in a tumor is one of the objects of target therapy. Due to cell interaction via signalling pathways or soluble factors induce tumor growth and drug resistance. Stromal cells, like a fibroblast, secrete many cytokines and growth factors [16, 17]. These molecules activate phosphatidylinositol-3-kinase (PI3K)/AKT and nuclear factor kappa light chain enhancer of activated B cells (NF- κ B) pathways in cancer cells and cause drug resistance in cancer cells [18]. Tumor microenvironment could affect drug resistance in cancer cells due to cell interaction. So, cell-cell interaction in cancer needs to be studied more

to understand this mechanism to prevent drug resistance in tumors.

This study aimed to evaluate cancer cell-cell interaction by isolating several phenotypically different cell sublines from the MDA-MB-231 cell line. Investigate the influence of these cell sublines interaction on resistance to anticancer drugs in 2D and 3D cell culture models. For subline characterization, we used immunocytochemistry and stained the cells with stem-like cancer cell (CSCs) CD133 antibody to investigate CD133 receptor expression in sublines. To assess the sublines' resistance to anticancer drugs, we applied the MTT cytotoxicity assay. A wound-healing assay was used to estimate the cell's ability to migrate. The most characteristic sublines D8, F5, H2 at drug sensitivity, migration, and CSCs-like properties, were chosen. Cell interaction research is performed by mixing these sublines in many ways: 1) sublines with fibroblast cells; 2) MDA-MB-231, fibroblasts and sublines; 3) mixing sublines between each other and fibroblasts. Interaction studies performed in 2D and 3D models.

Materials and methods

Cell culturing

Human triple-negative breast cancer cells MDA-MB-231 were obtained from the American Type Culture Collection (ATCC, Manassas, VA, USA). Human foreskin fibroblasts (HF) CRL-4001 were initially obtained from ATCC and kindly provided by Prof. Helder Santos (University of Helsinki, Finland). Cell lines were cultured in Dulbecco's Modified Eagle Medium (DMEM) GlutaMAX (Gibco, UK) supplemented with 10% fetal bovine serum (FBS, qualified, heat-inactivated, E.U.-approved, South America Origin, Gibco, UK), 10,000 U/ml penicillin, 10 mg/ml streptomycin (Gibco, UK), 1 μ g/ml insulin 27 USP units/mg (Gibco, UK), 1% minimum essential medium non-essential amino acids (MEM NEAA) (Gibco, UK), 1% sodium pyruvate (Gibco, UK). Cells were maintained in a humidified atmosphere containing 5% CO₂ at 37°C. The same conditions were used for the MDA-MB-231 isolated sublines.

Isolation of cell sublines from commercial MDA-MB-231 cell line

Cell sublines were isolated from the MDA-MB-231 commercial cell line by multiple cell

Interaction of phenotypic sublines isolated from MDA-MB-231 cell line

suspension dilution in 96-well plates. Using an 8-channel micropipettor, 100 μ l of medium was added to all the wells in 96-well plate, except well A1. Then 200 μ l of cell suspension (2×10^4 cell/ml) was added into well A1, and using a single channel pipettor, 100 μ l of the solution was quickly transferred from the first well to well B1. This dilution was repeated down the entire column, discarding 100 μ l from H1, so that it ends up with the same volume as the wells above it. With the 8-channel micro pipettor, 100 μ l of medium was added to each well in column 1 (giving 200 μ l/well). Using the same pipettor, 100 μ l of the liquid was quickly transferred from the wells in the first column (A1-H1) to those in the second column (A2-H2). This dilution strategy was repeated across the entire plate.

After nine days of incubation, the cell colonies in the plate were detected microscopically. Based on formed colonies differences (shape, density of cells), sublines from the wells A9, B7, C7, D8, E7, F5, F7, G5, and H2 were selected (the names of subcolonies were assigned according to the name of the well from which the cells were taken). Sublines were sub-cultured to 25 cm² cell culture flasks (TPP, Switzerland).

Expression of CD133 receptor by immunofluorescence staining

Cells (4×10^4 cell/ml) were grown for 24 h in a 24-well plate on collagen-coated oval 13 mm diameter cover glasses at standard cell culturing conditions. After 24 h, cells were fixed in 4% paraformaldehyde (Thermo Scientific, Waltham, Massachusetts, USA) for 20 min., permeabilized in 0.1% Triton X-100 (Thermo Scientific, Waltham, Massachusetts, USA) for 10 min., blocked in blocking buffer (10 ml of phosphate buffer solution + 0.2 ml fetal bovine serum + 0.02 g bovine serum albumin) for 30 min. Immunostaining was performed with primary antibody 1:50 (anti-CD133 rabbit polyclonal, Abcam, Cambridge, UK) against the protein CD133. Then cells were incubated with secondary antibody 1:1000 (goat anti-rabbit IgG highly cross-adsorbed secondary antibody, Alexa Fluor 594, life technologies, Oregon, USA) for 30 min. Cell nuclei were stained with DAPI (Thermo Scientific, Waltham, Massachusetts, USA) 1 μ g/ml, for 10 min. Then cover glass was

transferred to objective lenses and mounted in ProLong Gold Antifade reagent (Invitrogen, Carlsbad, California, USA). CD133 expression was determined by immunofluorescence using confocal microscopy (Olympus FLUOVIEW FV1000). Cells were imaged under a microscope at 600 \times magnification using DAPI and TRITC filters. Images were analyzed using ImageJ 1.53K software (National Institute of Health, Bethesda, Maryland, USA). In each group, at least 20 (from 5 different glass points) randomly selected cells were analyzed, and the relative fluorescence intensity was measured. HF cells were used as a negative control.

Wound healing assay

Cells were seeded in a 24-well plates (Corning, New York, USA) at a density of 20000 cells/well in 500 μ L of medium and incubated for 24 h in a humidified atmosphere containing 5% CO₂ at 37°C. Then the monolayers were scratched with a sterile 100 μ L pipette tip in the center of the well. The media was removed, cells were washed twice with PBS, and the fresh media was added. Images of the scratch were captured immediately and at every 24 h for three days at several well points of scratch. The percentage of the wound was calculated using ImageJ software (National Institute of Health, Bethesda, Maryland, USA). Three technical replicates per experiment were made.

Chemosensitivity assay

Cell susceptibility to anticancer drugs was established by MTT assay, as described elsewhere [19]. All drug dilutions in media were prepared freshly just before use. DOX (> 98%, Abcam, Cambridge, UK) and PTX (> 99.5% Alfa Aesar, Kandel, Germany) were dissolved in dimethyl sulfoxide (DMSO, Sigma-Aldrich Co, St. Louis, MO, USA) and diluted in medium (final DMSO concentration did not exceed 0.5%). Cells (5×10^3 cells/well) were plated into 96-well flat-bottomed plates and incubated for 24 h. Then the dilutions of drugs were added to each well. The only medium without cells was used as a positive control, and the medium with 0.5% DMSO served as a negative control. After three days of incubation, the medium was removed and 100 μ l of 3-(4,5-dimethylthiazol-2-yl)-2,5-diphenyltetrazdium bromide (MTT, Life technologies, Oregon, USA) solution (0.5 mg/ml

Interaction of phenotypic sublines isolated from MDA-MB-231 cell line

in medium) was added. After incubation for 3 h at 37°C, the liquid was discarded, and the formed formazan crystals were dissolved in 50 µl of DMSO. Complete solubilization of formazan crystals was achieved by short shaking. The absorbance was measured on a plate reader at 570 and 630 nm. EC_{50} values were calculated using Hill equation. Experiments were repeated three times.

Cell doubling time

Prepared cell suspension of 2×10^4 cells/ml was seeded in a 24-well plate (8×10^3 cells/well). After 24, 48, 72, and 96 h, cells were washed twice with PBS, trypsinized and centrifuged at 1000 rpm for 4 min. Then the cells were resuspended in 200 µl of fresh medium and counted in duplicates on a hemocytometer. Cell doubling time (DT) was estimated by the following formula (1) [18] to calculate each line and subline DT, where c_1 and c_2 are the number of cultured cells at the current (t_2) and previous (t_1).

$$DT = \frac{\ln(2) \times (t_2 - t_1)}{\ln\left(\frac{c_2}{c_1}\right)} \quad (1)$$

Spheroid formation and growth

Spheroids were formed from MDA-MB-231 line and sublines by the magnetic 3D Bioprinting method [21], as described elsewhere [20]. Cancer cells were mixed with human fibroblasts (1:1), to create a better-representing tumor microenvironment, as the noncancer cells, like fibroblasts, endothelial, immune cells (e.g., monocytes, neutrophils, and lymphocytes), and extracellular matrix components (e.g., proteoglycans, glycosaminoglycans, and collagens) play an essential role in cell signaling, tumor growth, and development [29]. The cells were incubated with nanoparticles NanoShuttle (Nano3D Biosciences Inc., Houston, TX, USA) for 8-10 h. Then cells were trypsinized and seeded into ultra-low attachment 96-well plates at a volume of 100 µL (2,000 breast cancer cells and 2,000 human fibroblasts per well). In all cell mixtures, the HF cells composed 50% of cells. The plate was placed on a magnetic drive and incubated in a humidified atmosphere containing 5% CO₂ at 37°C until spheroids were formed. After two days of incubation, the images of spheroids were taken every 48 h.

Before taking images, the medium was replaced by a fresh one containing 0.5 µM of DOX and 0.05 µM PTX. The spheroid size was calculated using ImageJ software (NIH).

Statistical analysis

All experiments were repeated three times, calculating the mean and standard deviation. The data were processed using Microsoft Office Excel 2016 software (Microsoft Corporation, Redmond, WA, USA) and IBM SPSS Statistics version 26.0 package. The level of statistical significance was set at $P < 0.05$. An analysis of variance (ANOVA) followed by a Tukey post-hoc test was performed to determine significant differences between values.

Results

Isolation of subpopulations within MDA-MB-231 cell line and their characterization

We isolated new sublines from the TNBC cell line MDA-MB-231 by multiple dilutions of the cell suspensions in a 96-well microplate [21]. After 7-14 days, colonies were formed, and seven colonies (sublines) were selected based on differences of colony density, size, and shape (**Figure 1**). These sublines showed a spectrum of morphologies ranging from round or oval colonies of closely packed cells to irregularly shaped colonies of loosely packed cells. The F5 and E7 sublines were non-elongated, shorter, and more oval, and the cells were tightly packed, forming colonies during cell growth; D8 and F7 - were more elongated in shape and comprised of loosely packed cells. The H2 subline cells were shorter in shape compared to parental cell line. The morphology of A9 and G5 was intermediate between the first and second groups of sublines. Differences in cell morphology are associated with their morphodynamics [22] - elongated cell shape related to increased migration and more aggressive cell phenotypes.

CD133 receptor expression in cell sublines

The CD133 antigen, also known as prominin-1, is a single-chain transmembrane glycoprotein identified as an important surface marker of breast cancer stem cells [23]. The expression of CD133 is dysregulated in various solid tumors, as well as TNBC and BRCA-1 tumors [24]. The specific function of CD133 in cancer

Interaction of phenotypic sublines isolated from MDA-MB-231 cell line

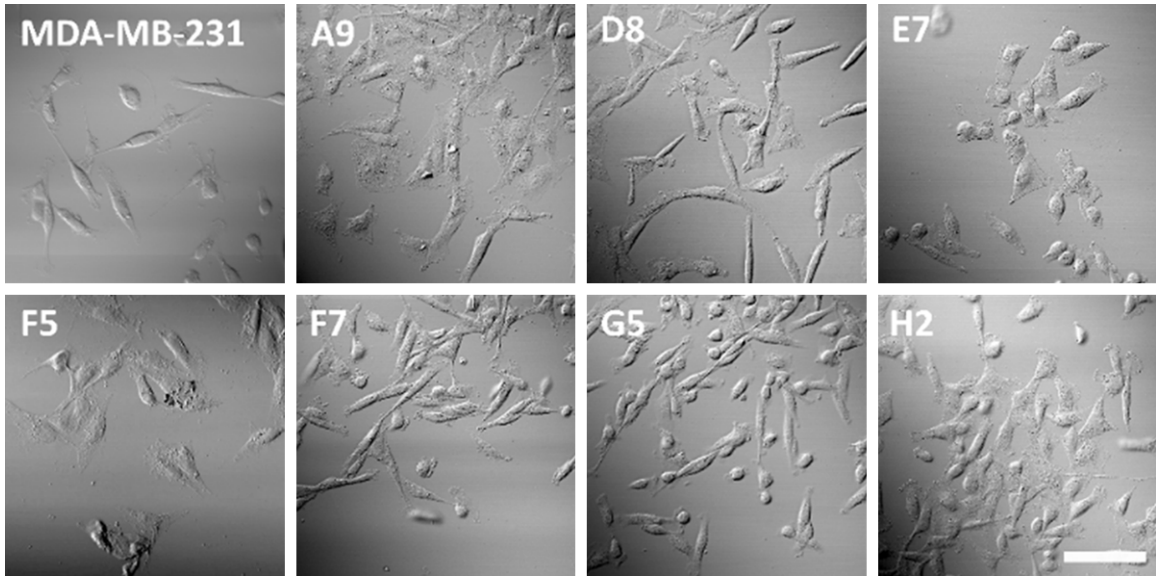


Figure 1. Morphological features of MDA-MB-231 cell lines and isolated sublines. The scale bar represents 50 μm .

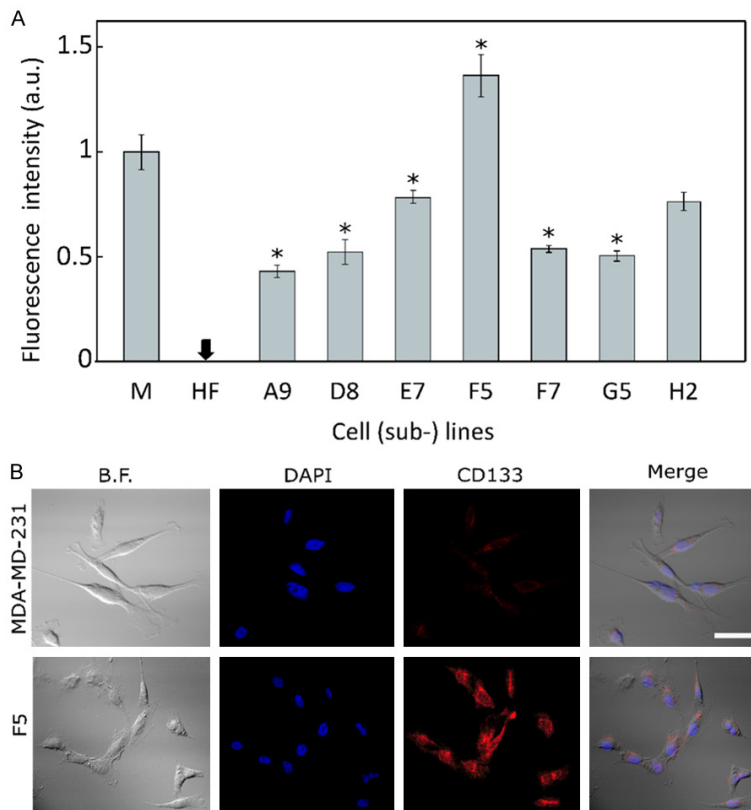


Figure 2. Immunofluorescence staining of CD133 in indicated cell lines and sublines. **A.** The quantified CD133 expression was different among cell (sub-)lines. The highest CD133 receptor expression was determined in subline F5 and the lowest in subline A9. **B.** Cells were labeled using anti-CD133 rabbit polyclonal primary antibody and goat anti-rabbit secondary antibody, Alexa Fluor 594 (red). Nuclei (blue) were stained with DAPI. The asterisk (*) indicates $P < 0.05$ compared to the control, $n = 3$, scale bar represents 50 μm . Abbreviations: M, MDA-MB-231 cell line.

cells has not been defined, but CD133 is accompanied by increased malignancy and multi-drug resistance by enhancing PI3K/Akt signalling in breast cancer cells [25]. Activating the PI3K/Akt signalling pathway in several human cancers, including breast cancer, induces cell proliferation, invasion, multidrug resistance, and metastasis of tumor cells [26-28]. The PI3K/Akt signalling was shown to promote the expression of a master transcription factor of epithelial-mesenchymal transition (EMT), leading to enhance TGF- β receptor signalling, which in turn functions to maintain hyperactivated PI3K/Akt signalling, cooperatively driving breast tumor metastasis [28]. The expression of CD133 in cancer-initiating cells has been reported in several tumor types, and recently CD133 was identified in breast CSCs [29]. We aimed to figure out this CSCs cell phenotype in our isolated cell sublines (Figure 2). For it we chose immunofluorescence method that can provide valuable com-

Interaction of phenotypic sublines isolated from MDA-MB-231 cell line

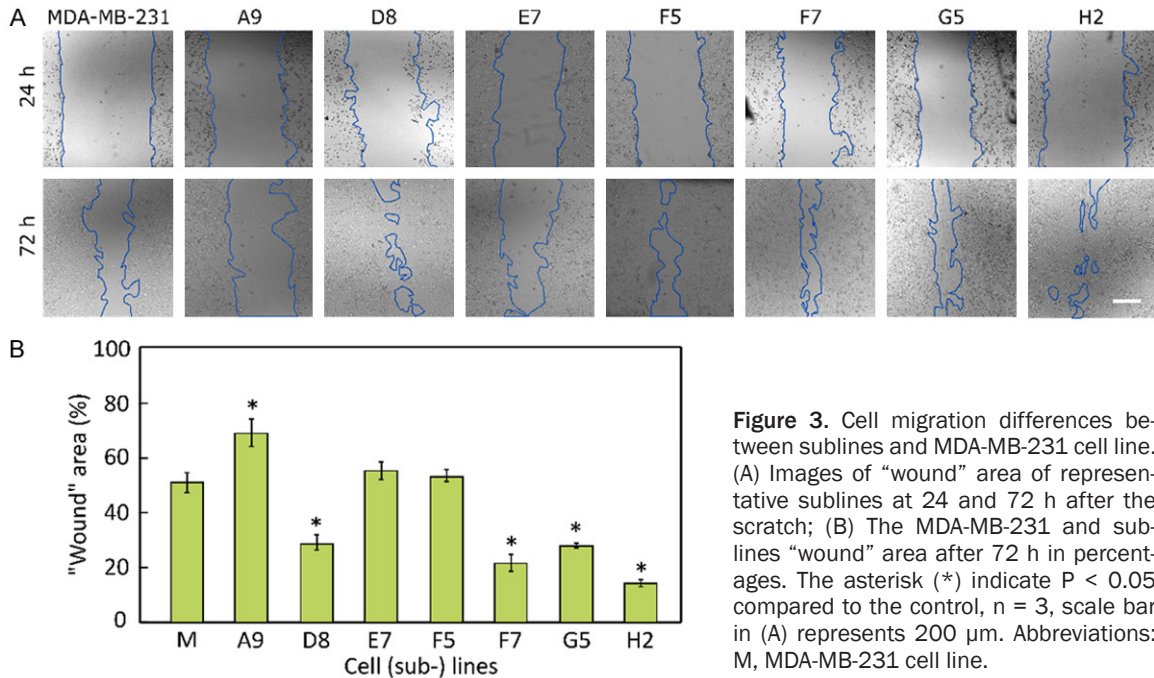


Figure 3. Cell migration differences between sublines and MDA-MB-231 cell line. (A) Images of "wound" area of representative sublines at 24 and 72 h after the scratch; (B) The MDA-MB-231 and sublines "wound" area after 72 h in percentages. The asterisk (*) indicate $P < 0.05$ compared to the control, $n = 3$, scale bar in (A) represents 200 μm . Abbreviations: M, MDA-MB-231 cell line.

plementary information, such as subcellular localization of CD133, morphological information about cells. CD133 receptors were not detected in the HF cell line (Figure 2A), which was used as a negative control. However, the subline F5 exhibited the highest CD133 expression compared to other sublines. CD133 expression in subline F5 was 31% higher than in the MDA-MB-231 commercial cell line. In other sublines: A9, D8, E7, F7, G5, and H2, fluorescence intensity was from 21% to 57% lower than in the MDA-MB-231 cell line.

The cell sublines' ability to migrate

Tumor cell migration is the most critical trait of metastasis. The differences between cell subline migration abilities were examined using a wound-healing assay (Figure 3). Analysis of the wound area changes shows different migration ability of cell sublines (Figure 3A). The slowest migration was determined for the A9 subline cells. The "wound" area after 72 h was 19% larger compared to the MDA-MB-231 "wound" area (Figure 3B). Furthermore, H2 subline cells migrated faster and the "wound" area after 72 h was 38% smaller than the MDA-MB-231 "wound" area. The other sublines - D8, F7, and G5 cells were also more migrant, and

the "wound" area after 72 h was from 20 to 30% smaller than MDA-MB-231 "wound" area.

Susceptibility to anticancer drugs

Cell (sub)lines susceptibility to anticancer drugs was evaluated by MTT assay. The results are shown in Figures 4 and 5. The subline H2 was about 1.5 times more resistant to DOX than the parent MDA-MB-231 cell line (Figure 4). EC_{50} value in H2 after 72 h was 175.4 ± 4.4 nM, whereas in MDA-MB-231 EC_{50} value was 126.7 ± 1.6 nM. Sublines E7, F5, and G5 were about twice more sensitive to DOX than the parent cell line (EC_{50} after 72 h were 77.7 ± 11.2 nM and 55.9 ± 7.2 nM, respectively). Subline D8 sensitivity to DOX was similar to MDA-MB-231 sensitivity. Among tested cell sublines, H2 had the highest resistance to PTX (Figure 5), EC_{50} after 72 h was 72.6 ± 2.1 nM, whereas EC_{50} in MDA-MB-231 was 55.2 ± 2.8 nM. Subline A9 was slightly more sensitive to PTX than the parental cell line, with EC_{50} 43.9 ± 1.8 nM, though this subline was resistant to DOX. The subline F7 was sensitive to PTX (EC_{50} 46.9 ± 4.5 nM). The sensitivity of sublines D8, E7, F5, and G5 was comparable to MDA-MB-231 sensitivity. The most resistant cell subline to both DOX and PTX was H2. The most sensitive

Interaction of phenotypic sublines isolated from MDA-MB-231 cell line

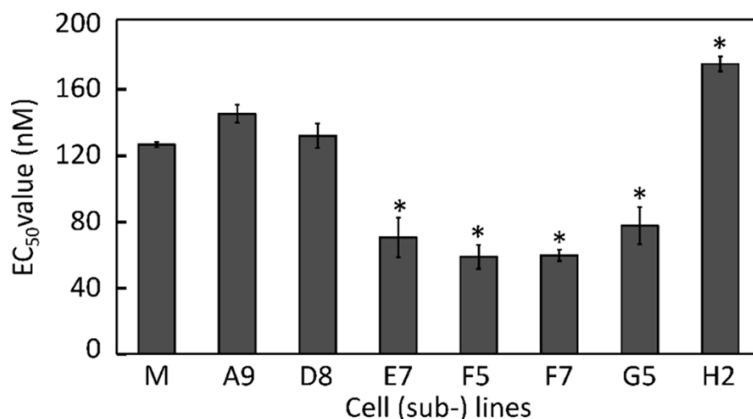


Figure 4. DOX effect on cell viability. The EC_{50} values of DOX after 72 h in breast cancer MDA-MB-231 cell line and isolated sublines. Abbreviations: EC_{50} , half maximal effective concentration; M, MDA-MB-231 cell line; The asterisks (*) indicate $P < 0.05$ compared to control, $n = 3$.

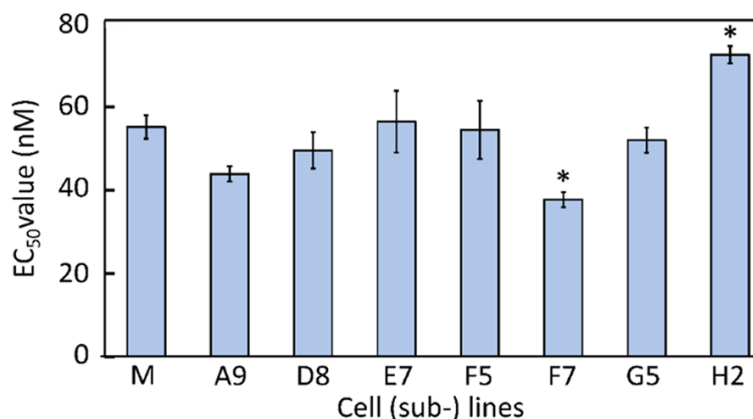


Figure 5. PTX effect on cell viability. The EC_{50} values of PTX after 72 h in breast cancer MDA-MB-231 cell line and isolated sublines. Abbreviations: EC_{50} , half maximal effective concentration; M, MDA-MB-231 cell line; The asterisks (*) indicate $P < 0.05$ compared to control, $n = 3$.

Table 1. Properties of selected sublines

Properties	D8	F5	H2
CD133 expression	50% L ¹	31% H	26% L
Ability to migrate	20% H ²	5% L	38% H
Sensitivity to DOX	4.2% H (NSD ³)	54% L	39% H
Sensitivity to PTX	10% L	1.3% L (NSD)	32% H

¹L - lower than control, ²H - higher than control, ³NSD - no significant difference. All experimental results compared to commercial cell line MDA-MB-231 results.

to DOX were sublines F5 and F7, and PTX - subline F7.

Selection of sublines for the interaction studies

We observed differences in receptor expression, migration ability, and their sensitivity to

anticancer drugs DOX and PTX. After all, we summarized all results and chose three the most characteristic sublines for further research (Table 1). Subline F5 cells were different in appearance compared with MDA-MB-231 cells. Cells formed compact colonies with typical epithelial polygonal shapes in close contact with each other. This subline was characterized by a higher expression of the CD133 receptor among all tested sublines (31% higher than in MDA-MB-231). The sensitivity of the F5 subline to PTX was not statistically significant, but the F5 subline cells were 50% more sensitive to anticancer compound DOX than the MDA-MB-231 cell line. The F5 subline cells migrated slower than the parental cell line.

The expression of CD133 in D8 subline cells was the lowest among all sublines and 50% lower than in the parental cell line. The D8 subline was 4.2% more resistant to DOX and 10% more sensitive to PTX than the parental cell line. The migration rate of the D8 subline was about 20% higher than that of the parental cell line.

The third subline, H2, was different from other sublines. The expression of CD133 in H2 was 26% lower than in the parental cell line. The H2 subline cells were 38% more resistant to DOX and 31% more resistant to PTX than the MDA-MB-231 line. The H2 subline cells migrated faster than the MDA-MB-231 cell line. These three sublines were chosen for further studies of cell interaction.

Doubling time of sublines

After the selection of three cell sublines (F5, D8, H2), at first, we focused on their cell dou-

Interaction of phenotypic sublines isolated from MDA-MB-231 cell line

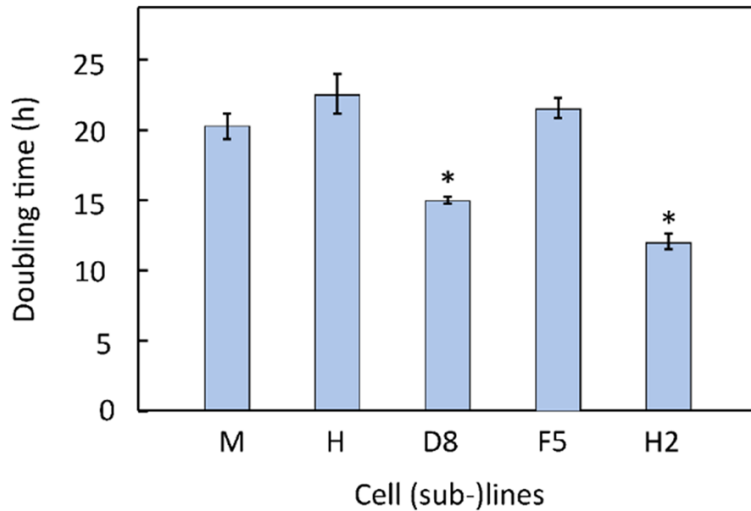


Figure 6. The doubling time of cell lines and sublines. The asterisks (*) indicate $P < 0.05$ compared to the control, MDA-MB-231, $n = 3$. Abbreviations: M, MDA-MB-231 cell line; H, HF cell line.

	Combination group I	Combination group II	Combination group III
Mixed with	+HF	+HF/+MDA	+HF/+sublines
cell mixtures	MDA/HF		
	D8/HF	D8/MDA/HF	D8/F5/HF
	F5/HF	F5/MDA/HF	D8/H2/HF
	H2/HF	H2/MDA/HF	F5/H2/HF

Figure 7. Combinations of cell lines and sublines used for interaction research. Abbreviations: MDA, MDA-MB-231 cell line.

bling time (DT) (**Figure 6**). The DT of MDA-MB-231 commercial cell line was about 20 h, and the DT of HF was approximately 22 h. DT of isolated sublines from the MDA-MB-231 commercial cell line was different. The F5 subline DT was 21 h, the D8 - 15 h, and H2 subline DT was 12 h. In summary, most isolated sublines were characterized by faster dividing cell phenotypes than the parent cell line.

Cell interaction studies in the 2D model

Cell sublines were selected to study the relevance of cell-cell communication *in vitro* studies. We made three cell subline mixtures for interaction research (**Figure 7**). First, we explored combinations of sublines and MDA-

MB-231 cell line mixed with HF (**Figure 7**, combination I). The second group (**Figure 7**, combination II) consisted of sublines (D8, F5, H2) combined with HF and MDA-MB-231 cells. The third group (**Figure 7**, combination III) consisted of two sublines (D8, F5 or D8, H2 or F5, H2) mixed with HF.

In cell interaction study, we used the HF cells to mimic the tumor microenvironment. It is known that the interaction between breast cancer cells and tumor microenvironments is essential for tumor growth and progression. Cells that support the function of epithelial cells, like cancer-associated fibroblasts (CAFs), contribute to therapy resistance via the production of several secreted factors and direct interaction with cancer cells [30-33]. The MDA-MB-231 cell line in combination II was used to evaluate the parental cell line and isolated sublines' interaction influence on drug resistance. The MDA-MB-231 cells are phenotypically different from each other [34] and have much more different phenotypes than we found. Additionally, we want to look up isolated sublines interaction with all populations in MDA-MB-231 cell line. By combining two (combination III) different sublines together (D8, F5 or D8, H2 or F5, H2), we assess the influence of the interaction of cells with different characteristics to evaluate drug resistance in these combinations. All tested cell combinations showed different responses to drugs DOX and PTX (**Figure 8**).

We used the same concentration of DOX (0.5 μM) and PTX (0.05 μM) in all tested cell combinations. Concentrations were chosen based on previous experiments of EC_{50} . MTT assay was chosen due to its simplicity, and it allowed us to assess the overall viability of the cell com-

Interaction of phenotypic sublines isolated from MDA-MB-231 cell line

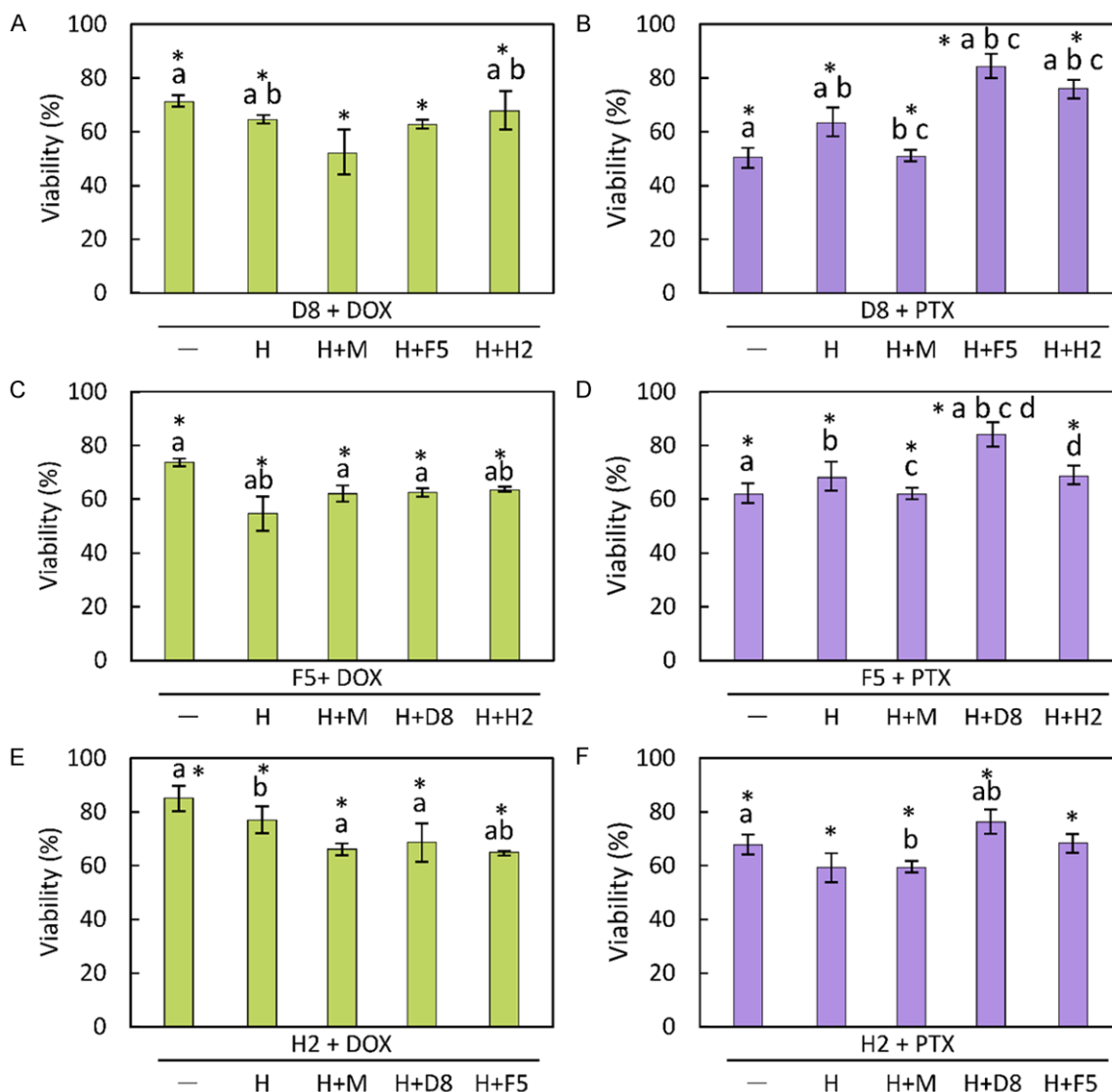


Figure 8. The cell susceptibility to anticancer drugs DOX and PTX. The percentage of cell viability after 72 h treatment in D8 cells combinations with DOX (A) and PTX (B), F5 cells combinations with DOX (C) and PTX (D), H2 cells combination with DOX (E) and PTX (F). The “-” symbol on the x-axis indicates that no additional cells were added. The asterisk (*) indicate $P < 0.05$ compared to the control (control group consisted of cells treated with DMSO). Bars marked with different letters indicate statistically significant differences ($P < 0.05$) within the same category. Abbreviations: M, MDA-MB-231 cell line; H, HF cell line; n = 3.

binations in rapid manner and evaluate cell combination viability as a whole. This method in 2D model studies required minimal additional optimization. The DOX resistance in D8, F5, and H2 sublines (Figure 8A, 8C, 8E) was observed, and cell viability after 72 h treatment with DOX varied from 72% to 85%. These sublines in combination with HF or MDA-MB-231 or each other, possessed lower resistance to DOX, it decreased by 9 to 16% compared with separate sublines. The opposite results were

observed in the case of cell combination response to PTX (Figure 8B, 8D, 8F). In cell sublines combined with HF or MDA-MB-231 or with each other, the resistance to PTX increased by 18-34% compared to the separate sublines.

Cell interaction studies in the 3D model

Nowadays, 3D cultures are widely used to study the effects of new compounds or anticancer drugs [35]. Magnetic 3D bioprinting method

Interaction of phenotypic sublines isolated from MDA-MB-231 cell line

advantages in reproducibility, control over spheroid formation, and the ability to incorporate multiple cell types. The method is also simple, scalable, we can use any drug and any cell combinations to form spheroids and evaluate cell interaction influence on resistance or sensitivity to drugs and a whole spheroid size change. We applied 3D model to explore cell-cell interaction as it better represents the real tumor microenvironment. We used the same cell combinations as in the 2D model. The sublines alone were not included in these experiments, as TNBC cells without HF did not form spheroids.

The spheroids of the D8 and HF cells combinations (**Figure 9A, 9B**) were more sensitive to PTX treatment, and their size after 12 days was about 5% lower compared with the control. The spheroids formed from D8, HF and H2 subline cells were more sensitive to DOX and PTX. Spheroid size after 12 days was from 18% to 24% lower, respectively, compared to the control. The spheroid size of the F5, HF, and MDA-MB-231 cell combinations (**Figure 9C, 9D**) in the presence of PTX after 12 days was 7% bigger compared to the control. Spheroids composed from F5, HF, and H2 subline cells in the presence of DOX or PTX in a medium, were from 15% to 29% smaller after 12 days, respectively, compared to control (**Figure 9E, 9F**).

In 3D cell interaction study, we established that sublines D8, F5 cell interaction with subline H2 cells reduced their resistance to DOX and PTX compared to the control. The spheroids, which consisted of subline H2 cells, grew smaller in size compared to other tested groups.

Discussion

This study evaluated an interaction influence on drug resistance of different cell phenotypes isolated from the MDA-MB-231 cell line. We isolated seven new sublines from the MDA-MB-231 cell line, and three of them (D8, F5, H2) for cell interaction studies were chosen. These sublines differed from the others in the expression of the CD133 receptor, susceptibility to anticancer drugs, and ability to migrate.

CD133 is an important biomarker to identify and isolate the specific cell subpopulation named "cancer stem cells" (CSCs) in breast cancer. CSCs are a small cell population caus-

ing therapeutic resistance, metastasis, and recurrence of tumors, and might be used as the target of cancer treatment [36, 37]. CD133-positive cells have stemness properties such as drug resistance, self-renewal, differentiation ability, and high proliferation, and they are more resistant to standard chemotherapy [38]. During the immunofluorescence assay, we confirmed the existence, in MDA-MB-231 cells, of a small subpopulation (named F5) expressing a high level of CD133 in both membrane and cytoplasm compartments. We are not the first who found CD133 positive cell subpopulation in the MDA-MB-231 cell line. The first time CD133 was identified in 1997 [39], many scientists found some subpopulations of CD133-positive cells in the MDA-MB-231 cell line. The scientist also notes that these subpopulations cells showed enhanced cell growth, migration, drug resistance and invasion [40-42]. Our study found that the F5 subline possesses a 31% higher CD133 receptor expression than the commercial MDA-MB-231 cell line (**Figure 2B**). We hypothesized that the F5 subline would exhibit resistance to DOX and PTX, but it was two times more sensitive to DOX than the commercial cell line, and susceptibility to PTX was not statistically significantly different from the control. Many scientists found CD133-positive cells association to drug resistance [44] but exist several resistance mechanisms. First, CD133 overexpression in cancer cells activates PI3K/Akt, AKT/Wnt and other signalling pathways and affects the behaviour of CD133 cells, thereby playing a major role in cancer therapy [43]. Second, CD133 regulates tumor resistance via the AKT/NF- κ B/multidrug resistance protein (MDR)1 pathway [44]. Third, the high expression of CD133 is associated with drug resistance due to increased ABC transporter ABCG2, resulting in breast cancer resistance for platinum, paclitaxel [45] and doxorubicin [46].

We have a hypothesis that in our isolated F5 subline cells the MDR pumps gene was not activated and that has been cause cells sensitivity for DOX and PTX. Also, F5 subline cells didn't show increased migration rates compared with the control (**Figure 3**). It could be related to the heterogeneity of CD133 expression in the MDA-MB-231 cell line, where not all subpopulations showed the same expression level of CD133 [47]. Moreover, the F5 subline in

Interaction of phenotypic sublines isolated from MDA-MB-231 cell line

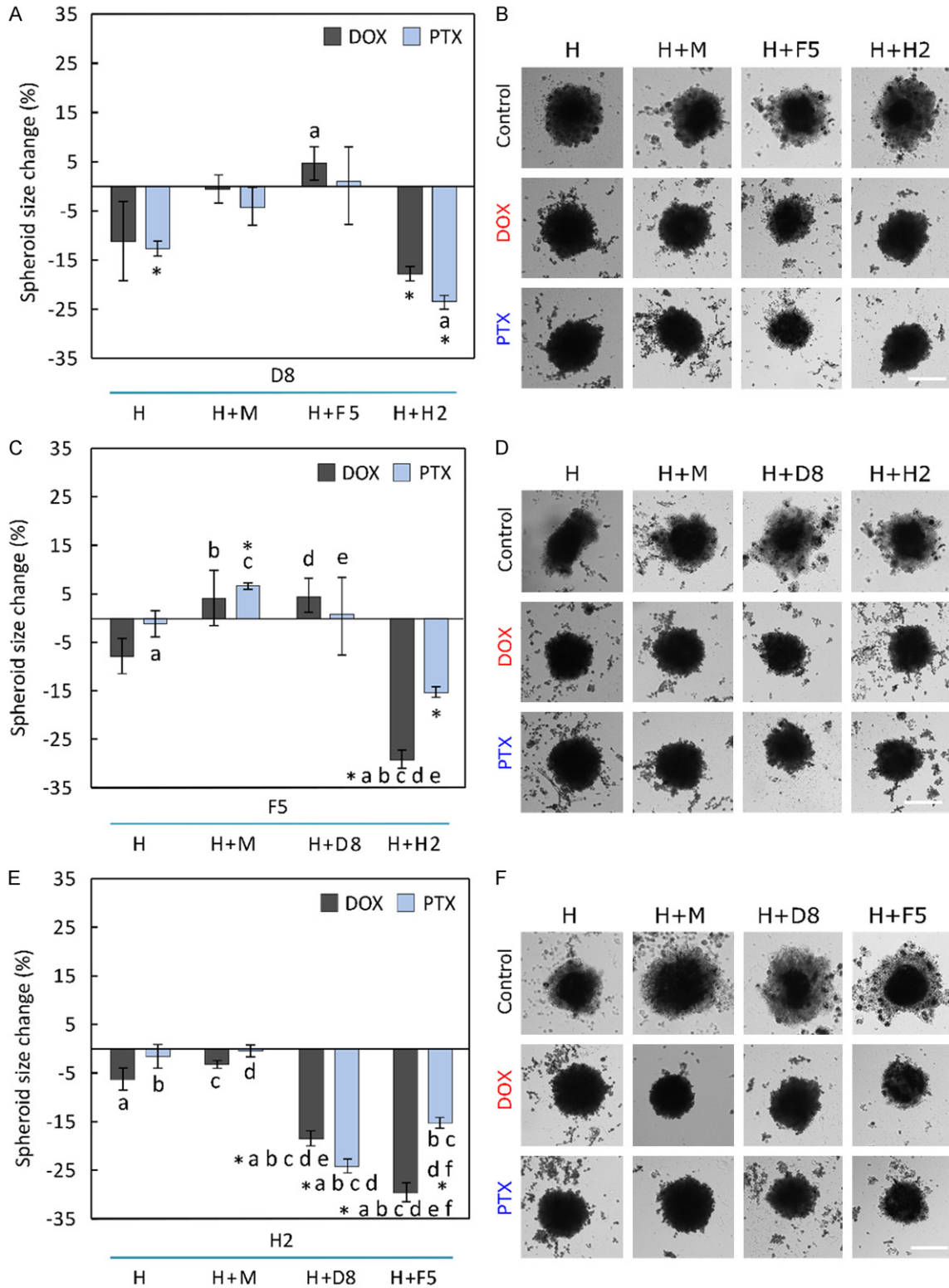


Figure 9. Effect of cell sublines combinations in 3D cultures. The percentage of spheroid size changes after 12 days of incubation with DOX and PTX compared to the control. D8 subline combinations (A, B), F5 subline combinations (C, D) and H2 subline combinations (E, F). The asterisks (*) indicate $P < 0.05$ compared to control (control group consisted of spheroids treated with DMSO). Bars marked with different letters indicate statistically significant differences ($P < 0.05$) within the same category. Abbreviations: M, MDA-MB-231 cell line; H, HF cell line; $n = 2$, scale bar 200 μM .

Interaction of phenotypic sublines isolated from MDA-MB-231 cell line

the 3D model was more resistant to DOX and PTX in both alone with HF and in combinations with other sublines. Scientists observed that due to cell-cell interaction in 3D cultures, several molecules (HGF, TGF β , VEGF, TNF α , FGF2, IL-6 and IL-8) are secreted in higher concentrations from fibroblasts cells. Also, scientists found that in 3D culture of fibroblasts results in an increased secretion of signaling molecules compared to stromal fibroblasts cultured in 2D, which provides that the 3D environment affected stromal fibroblasts. The fibroblast cells' functional differences in 2D vs. 3D conditions were observed, specifically, the expression of HGF, which increases cancer cell transition from local carcinoma cells to invasive carcinoma cells and causes cancer resistance to treatment [48]. Another hypothesis could be that CD133 expression changes in F5 subline over time, we took a CD133 immunofluorescence experiments several times and one of them was 6 months after subline isolation. The significant CD133 expression changes in cell sublines were not observed. Also, we check publications and found that some genes (about 16 different genes), for example TRIM28 are involved in CD133 expression regulation. In cancer cells CD133 expression increased during cell proliferation and tumor cell growth [10, 11]. In other publication we found that CD133 expression increased in several ovarian cancer cells lines during cell spheres formation [12]. That could be the explanation why F5 subline in 2D cultures were more sensitive to anticancer compounds compared to the 3D cultures results.

The subline H2 was identified as an increased migration and drug-resistant phenotype. H2 cells showed a more remarkable migration ability than the MDA-MB-231 cell line, and this could be related to faster DT (12 h) than MDA-MB-231 DT (20 h) (**Figure 6**). The subline H2 cells were more resistant to drugs than the MDA-MB-231 cell line. Similarly, Amaro and colleagues isolated an increased migration subpopulation from the MDA-MB-231 cell line. This increased migration cell phenotype was more resistant to PTX than MDA-MB-231 cell line resistance to this compound [41]. In our research, we observed increased resistance to both DOX and PTX anticancer drugs. Interestingly, the CD133 marker expression in H2 subline is not a statistically significant differ-

ence compared with the control. So, resistance to drugs was due to other resistance mechanisms, for example, MDR pumps, drug inactivation, reduced absorption of drugs, changed drug metabolism and others [49]. Usually, increased cell migration is associated with increased expression of MDR pumps, and it causes resistance to DOX and PTX [50].

We found that subline D8 was also identified with increased migration capacity compared with the control. This subline (D8) showed decreased sensitivity to PTX and increased sensitivity to DOX. The relationship between PTX resistance and increased migration could explain the D8 subline-specific properties. Scientists found out that in PTX-resistant cancer cells cathepsin L (cysteine protease associated with cancer cell migration) undergoes that subsequently mediates mesenchymal phenotype of cancer cells via EMT induction and that induce cell migration [51, 52].

After we chose three phenotypic different cell sublines, we moved on to our main aim - the influence of cell-cell interaction on drug resistance. It is known that cell-to-cell communication is critical during tumor development and progression, allowing cancer cells to reprogram the surrounding tumor microenvironment [53]. Stromal cells usually interact with breast cancer cells through IL-6 and chemokine ligand 7 (CXCL7) secretion [54]. Here, stromal cells secrete IL-6 has an important role in acquired breast cancer chemoresistance, which promotes cell proliferation and CXCL7 responsible for the self-renewal potential of breast cancer cells [55]. In addition, IL-6 has proven protective effects against paclitaxel and doxorubicin in breast cancer cells [56]. These cytokines (IL-6 and CXCL7) activate PI3K/AKT (induce cell proliferation, invasion, multidrug resistance [27]) and NF- κ B (mediates cancer cell proliferation, survival and angiogenesis [57]) signaling pathways. Moreover, fibroblast secreted chemokine ligand 1, and IL-8 cytokines enhance expression of ABCG2 (known as breast cancer resistance ATP-binding cassette transporter, BRCP) and it is responsible for efflux of doxorubicin and causes resistance to this drug [58, 59]. The transforming growth factor β (TGF- β) is another factor secreted by fibroblasts and it signals a pathway that can trigger cell epithelial to mesenchymal transition (EMT). Thus, TGF- β

Interaction of phenotypic sublines isolated from MDA-MB-231 cell line

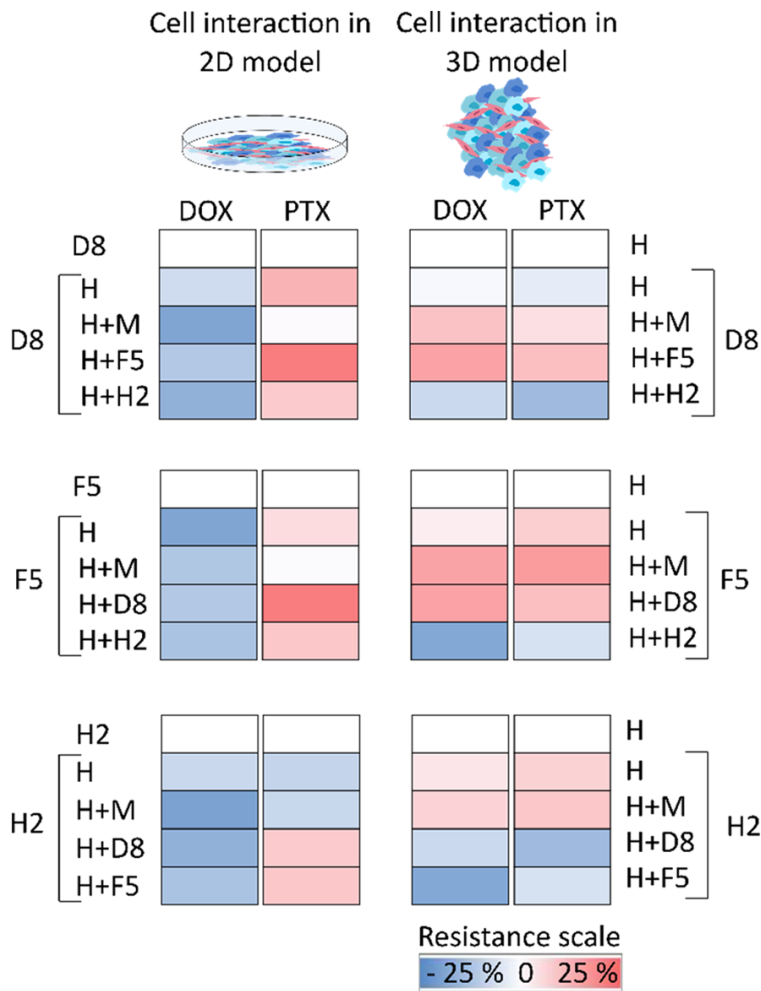


Figure 10. Summary of all cell sublines interaction research. Heatmap representation of cell combinations interaction influence on drug presence. Resistance scale (blue decreased resistance, red increased resistance) show how much combinations was resistant for drugs in percent.

contributes to the fibroblast's drug protective effect by inducing EMT. Also, fibroblast secreted factors such as CXCL12, FGF, HGF, IGF, PDGF, Wnt, MMPs, VEGF [54, 60] and these molecules activate, PI3K/AKT (promote the expression of a master transcription factor of epithelial-mesenchymal transition (EMT)) and NF- κ B pathways [61].

Fibroblast and breast cancer cell interaction due to various molecular mechanisms cause cancer cell drug resistance in both cell lines and tumors and disease progression in tumor. We found that fibroblasts alter the drug sensitivity of tumor cells in cell sublines-fibroblast-DOX and H2-fibroblast-PTX combination in 2D (Figure 8A, 8C, 8E), where more sensitive to drugs compared with sublines resistance al-

one. Moreover, F5-fibroblast-PTX and D8-fibroblast-PTX combinations (Figure 9B, 9D) were more resistant to PTX compared to sublines viability in monoculture. The same cancer-fibroblast-drug combination interaction effect was observed in Landry and colleagues' research [62] where resistance or sensitivity to drugs depends on the cancer and fibroblast cell phenotypes. In several studies, cancer cell-fibroblast interaction decreased drug resistance [63, 64], but in many cases, interaction with fibroblast induced drug resistance [65, 66]. In 3D model comparison, at sublines cell-fibroblast-drug combinations, drug resistance decreases (Figure 9). We also found out drug sensitivity differences in between sublines cell-drug combinations in 2D and 3D models. All sublines' combinations were sensitive to DOX but decreased sensitivity to PTX in 2D, especially in the combination of D8-F5-fibroblast-PTX (Figure 10). Moreover, in 3D model sublines cells between-fibroblast-drug, all combinations decrease sensitivity to DOX and PTX, except combinations with the H2 subline. A largescale study also observed that in a 3D model, TNBC cells-fibroblast-drug combination strongly altered drug sensitivity [62] and subtype-specific responses to treatment are not cell-intrinsic properties but rather a product of subtype-specific interactions between tumor cells and microenvironmental features.

Conclusions

Interaction between F5 (stem-like phenotype) and D8 (increased migration phenotype) sublines increased resistance to PTX in 2D cultures and resistance to both compounds in 3D cultures. The H2 subline which alone is the most resistant to DOX and PTX, interaction with other sublines decreased resistance to DOX in 2D

Interaction of phenotypic sublines isolated from MDA-MB-231 cell line

and in 3D to both compounds. In summary, we found that different phenotypes cancer cell interaction has a value influence of drug resistance and in some combination of cells reduced drug resistance. Therefore, future studies should aim to understand the mechanisms of interaction between cancer subline-subline and fibroblast-subline cells. In particular, the mechanisms by which different sublines phenotypes and fibroblasts alter the priming state of cancer cells.

Acknowledgements

This research was supported by the Science Foundation of Lithuania University of Health Sciences project “Implication of interactions between triple-negative breast cancer cell populations for chemotherapy resistance”, 2019.

Disclosure of conflict of interest

None.

Address correspondence to: Vilma Petrikaitė, Laboratory of Drug Targets Histopathology, Institute of Cardiology, Lithuanian University of Health Sciences, Sukileliu pr. 13, LT-50162, Kaunas, Lithuania. Tel: +370-686-29383; E-mail: vilma.petrikaite@ismuni.lt

References

- [1] Sung H, Ferlay J, Siegel RL, Laversanne M, Soerjomataram I, Jemal A and Bray F. Global cancer statistics 2020: GLOBOCAN estimates of incidence and mortality worldwide for 36 cancers in 185 countries. *CA Cancer J Clin* 2021; 71: 209-249.
- [2] Gnant M, Thomssen C and Harbeck N. St. Gallen/Vienna 2015: a brief summary of the consensus discussion. *Breast Care (Basel)* 2015; 10: 124-130.
- [3] Dent R, Trudeau M, Pritchard KI, Hanna WM, Kahn HK, Sawka CA, Lickley LA, Rawlinson E, Sun P and Narod SA. Triple-negative breast cancer: clinical features and patterns of recurrence. *Clin Cancer Res* 2007; 13: 4429-4434.
- [4] Lehmann BD, Bauer JA, Chen X, Sanders ME, Chakravarthy AB, Shyr Y and Pietenpol JA. Identification of human triple-negative breast cancer subtypes and preclinical models for selection of targeted therapies. *J Clin Invest* 2011; 121: 2750-2767.
- [5] Ahn SG, Kim SJ, Kim C and Jeong J. Molecular classification of triple-negative breast cancer. *J Breast Cancer* 2016; 19: 223-230.
- [6] Yam C, Mani SA and Moulder SL. Targeting the molecular subtypes of triple negative breast cancer: understanding the diversity to progress the field. *Oncologist* 2017; 22: 1086-1093.
- [7] Lehmann BD and Pietenpol JA. Identification and use of biomarkers in treatment strategies for triple negative breast cancer subtypes. *J Pathol* 2014; 232: 142-150.
- [8] Hubalek M, Czech T and Müller H. Biological subtypes of triple-negative breast cancer. *Breast Care (Basel)* 2017; 12: 8-14.
- [9] Burstein MD, Tsimelzon A, Poage GM, Covington KR, Contreras A, Fuqua SA, Savage MI, Osborne CK, Hilsenbeck SG, Chang JC, Mills GB, Lau CC and Brown PH. Comprehensive genomic analysis identifies novel subtypes and targets of triple-negative breast cancer. *Clin Cancer Res* 2015; 21: 1688-1698.
- [10] Wauters E and Vansteenkiste J. Will liquid biopsies become our fluid transition to personalized immunotherapy? *Ann Oncol* 2018; 29: 11-13.
- [11] Stanta G and Bonin S. A practical approach to tumor heterogeneity in clinical research and diagnostics. *Pathobiol* 2018; 85: 7-17.
- [12] Stanta G, Jahn SW, Bonin S and Hoefler G. Tumour heterogeneity: principles and practical consequences. *Virchows Arch* 2016; 469: 371-384.
- [13] Bonnefoi H, Grellety T, Tredan O, Saghatchian M, Dalenc F, Mailliez A, L'Haridon T, Cottu P, Abadie-Lacourtoisie S, You B, Mousseau M, Dauba J, Del Piano F, Desmoulins I, Coussy F, Madranges N, Grenier J, Bidard FC, Proudhon C, MacGrogan G, Orsini C, Pulido M and Gonçalves A. A phase II trial of abiraterone acetate plus prednisone in patients with triple-negative androgen receptor positive locally advanced or metastatic breast cancer (UCBG 12-1). *Ann Oncol* 2016; 27: 812-818.
- [14] Costa RLB and Gradishar WJ. Triple-negative breast cancer: current practice and future directions. *J Oncol Pract* 2017; 13: 301-303.
- [15] Nussinov R, Tsai CJ and Jang H. Anticancer drug resistance: an update and perspective. *Drug Resist Updat* 2021; 59: 100796.
- [16] Fitzgerald AA and Weiner LM. The role of fibroblast activation protein in health and malignancy. *Cancer Metastasis Rev* 2020; 39: 783-803.
- [17] Liu T, Han C, Wang S, Fang P, Ma Z, Xu L and Yin R. Cancer-associated fibroblasts: an emerging target of anti-cancer immunotherapy. *J Hematol Oncol* 2019; 12: 86.
- [18] Hemmings BA and Restuccia DF. PI3K-PKB/Akt pathway. *Cold Spring Harb Perspect Biol* 2012; 4: a011189.
- [19] Čeponytė U, Paškevičiūtė M and Petrikaitė V. Comparison of NSAIDs activity in COX-2 expressing and non-expressing 2D and 3D pancreatic cancer cell cultures. *Cancer Manag Res* 2018; 10: 1543-1551.

Interaction of phenotypic sublines isolated from MDA-MB-231 cell line

- [20] Bytautaite M and Petrikaite V. Comparative study of lipophilic statin activity in 2D and 3D in vitro models of human breast cancer cell lines MDA-MB-231 and MCF-7. *Onco Targets Ther* 2020; 13: 13201-13209.
- [21] Ye M, Wilhelm M, Gentschev I and Szalay A. A modified limiting dilution method for monoclonal stable cell line selection using a real-time fluorescence imaging system: a practical workflow and advanced applications. *Methods Protoc* 2021; 4: 16.
- [22] Qing Y, Yang XQ, Zhong ZY, Lei X, Xie JY, Li MX, Xiang DB, Li ZP, Yang ZZ, Wang G and Wang D. Microarray analysis of DNA damage repair gene expression profiles in cervical cancer cells radioresistant to 252 Cf neutron and X-rays. *BMC Cancer* 2010; 10: 71.
- [23] DA Cruz Paula A and Lopes C. Implications of different cancer stem cell phenotypes in breast cancer. *Anticancer Res* 2017; 37: 2173-2183.
- [24] Li GW and Xie XS. Central dogma at the single-molecule level in living cells. *Nature* 2011; 475: 308-315.
- [25] Li Z. CD133: a stem cell biomarker and beyond. *Exp Hematol Oncol* 2013; 2: 17.
- [26] Vivanco I and Sawyers CL. The phosphatidylinositol 3-Kinase-AKT pathway in human cancer. *Nat Rev Cancer* 2002; 2: 489-501.
- [27] Dong C, Wu J, Chen Y, Nie J and Chen C. Activation of PI3K/AKT/mTOR pathway causes drug resistance in breast cancer. *Front Pharmacol* 2021; 12: 628690.
- [28] Ortega MA, Fraile-Martínez O, Asúnsolo Á, Bujan J, Honduvilla N and Coca S. Signal transduction pathways in breast cancer: the important role of PI3K/Akt/mTOR. *J Oncol* 2020; 2020: 9258396.
- [29] Eddy CZ, Raposo H, Manchanda A, Wong R, Li F and Sun B. Morphodynamics facilitate cancer cells to navigate 3D extracellular matrix. *Sci Rep* 2021; 11: 20434.
- [30] Fernández-Nogueira P, Fuster G, Gutierrez-Uzquiza Á, Gascon P, Carbo N and Bragado P. Cancer-associated fibroblasts in breast cancer treatment response and metastasis. *Cancers (Basel)* 2021; 13: 3146.
- [31] Czekay RP, Cheon DJ, Samarakoon R, Kutz SM and Higgins PJ. Cancer-associated fibroblasts: mechanisms of tumor progression and novel therapeutic targets. *Cancers (Basel)* 2022; 14: 1231.
- [32] Louault K, Bonneaud TL, Séveno C, Gomez-Bougie P, Nguyen F, Gautier F, Bourgeois N, Loussouarn D, Kerdraon O, Barillé-Nion S, Jézéquel P, Campone M, Amiot M, Juin PP and Souazé F. Interactions between cancer-associated fibroblasts and tumor cells promote MCL-1 dependency in estrogen receptor-positive breast cancers. *Oncogene* 2019; 38: 3261-3273.
- [33] Mao X, Xu J, Wang W, Liang C, Hua J, Liu J, Zhang B, Meng Q, Yu X and Shi S. Crosstalk between cancer-associated fibroblasts and immune cells in the tumor microenvironment: new findings and future perspectives. *Mol Cancer* 2021; 20: 131.
- [34] Shen Y, Schmidt BUS, Kubitschke H, Morawetz EW, Wolf B, Käs JA and Losert W. Detecting heterogeneity in and between breast cancer cell lines. *Cancer Converg* 2020; 4: 1.
- [35] In: Fontana F, Santos HA, editors. *Bio-nanomedicine for cancer therapy*. Cham: Springer International Publishing; 2021. pp. 1295.
- [36] Morata-Tarifa C, Jiménez G, García MA, Entrena JM, Griñán-Lisón C, Aguilera M, Picon-Ruiz M and Marchal JA. Low adherent cancer cell subpopulations are enriched in tumorigenic and metastatic epithelial-to-mesenchymal transition-induced cancer stem-like cells. *Sci Rep* 2016; 6: 18772.
- [37] Freischel AR, Damaghi M, Cunningham JJ, Ibrahim-Hashim A, Gillies RJ, Gatenby RA and Brown JS. Frequency-dependent interactions determine outcome of competition between two breast cancer cell lines. *Sci Rep* 2021; 11: 4908.
- [38] Irollo E and Pirozzi G. CD133: to be or not to be, is this the real question? *Am J Transl Res* 2013; 5: 563-581.
- [39] Weigmann A, Corbeil D, Hellwig A and Huttner WB. Prominin, a novel microvilli-specific polytopic membrane protein of the apical surface of epithelial cells, is targeted to plasmalemmal protrusions of non-epithelial cells. *Proc Natl Acad Sci U S A* 1997; 94: 12425-12430.
- [40] Brugnoli F, Grassilli S, Piazzi M, Palomba M, Nika E, Bavelloni A, Capitani S and Bertagnolo V. In triple negative breast tumor cells, PLC-β2 promotes the conversion of CD133high to CD133low phenotype and reduces the CD133-related invasiveness. *Mol Cancer* 2013; 12: 165.
- [41] Brugnoli F, Grassilli S, Al-Qassab Y, Capitani S and Bertagnolo V. CD133 in breast cancer cells: more than a stem cell marker. *J Oncol* 2019; 2019: 7512632.
- [42] Croker AK, Goodale D, Chu J, Postenka C, Hedley BD, Hess DA and Allan AL. High aldehyde dehydrogenase and expression of cancer stem cell markers selects for breast cancer cells with enhanced malignant and metastatic ability. *J Cell Mol Med* 2009; 13: 2236-2252.
- [43] Manoranjan B, Chokshi C, Venugopal C, Subapanditha M, Savage N, Tatari N, Provias JP, Murty NK, Moffat J, Doble BW and Singh SK. A CD133-AKT-Wnt signaling axis drives glioblastoma brain tumor-initiating cells. *Oncogene* 2020; 39: 1590-1599.
- [44] Yuan Z, Liang X, Zhan Y, Wang Z, Xu J, Qiu Y, Wang J, Cao Y, Le VM, Ly HT, Xu J, Li W, Yin P and Xu K. Targeting CD133 reverses drug-resistance via the AKT/NF-κB/MDR1 pathway in colorectal cancer. *Br J Cancer* 2020; 122: 1342-1353.

Interaction of phenotypic sublines isolated from MDA-MB-231 cell line

- [45] Li Y, Wang Z, Ajani JA and Song S. Drug resistance and cancer stem cells. *Cell Commun Signal* 2021; 19: 19.
- [46] Mirzaei S, Gholami MH, Hashemi F, Zabolian A, Farahani MV, Hushmandi K, Zarrabi A, Goldman A, Ashrafizadeh M and Orive G. Advances in understanding the role of P-gp in doxorubicin resistance: Molecular pathways, therapeutic strategies, and prospects. *Drug Discov Today* 2022; 27: 436-455.
- [47] Tay ASS, Amano T, Edwards LA and Yu JS. CD133 mRNA-transfected dendritic cells induce coordinated cytotoxic and helper T cell responses against breast cancer stem cells. *Mol Ther Oncolytics* 2021; 22: 64-71.
- [48] Sung KE, Su X, Berthier E, Pehlke C, Friedl A and Beebe DJ. Understanding the impact of 2D and 3D fibroblast cultures on in vitro breast cancer models. *PLoS One* 2013; 8: e76373.
- [49] Mansoori B, Mohammadi A, Davudian S, Shirjang S and Baradaran B. The different mechanisms of cancer drug resistance: a brief review. *Adv Pharm Bull* 2017; 7: 339-348.
- [50] Kryczka J and Boncela J. Cell migration related to MDR-another impediment to effective chemotherapy? *Molecules* 2018; 23: 331.
- [51] Ashrafizadeh M, Mirzaei S, Hashemi F, Zarrabi A, Zabolian A, Saleki H, Sharifzadeh SO, Soleymani L, Daneshi S, Hushmandi K, Khan H, Kumar AP, Aref AR and Samarghandian S. New insight towards development of paclitaxel and docetaxel resistance in cancer cells: EMT as a novel molecular mechanism and therapeutic possibilities. *Biomed Pharmacother* 2021; 141: 111824.
- [52] Han ML, Zhao YF, Tan CH, Xiong YJ, Wang WJ, Wu F, Fei Y, Wang L and Liang ZQ. Cathepsin L upregulation-induced EMT phenotype is associated with the acquisition of cisplatin or paclitaxel resistance in A549 cells. *Acta Pharmacol Sin* 2016; 37: 1606-1622.
- [53] Chiodoni C, Di Martino MT, Zazzeroni F, Caraglia M, Donadelli M, Meschini S, Leonetti C and Scotlandi K. Cell communication and signaling: how to turn bad language into positive one. *J Exp Clin Cancer Res* 2019; 38: 128.
- [54] Korkaya H, Liu S and Wicha MS. Breast cancer stem cells, cytokine networks, and the tumor microenvironment. *J Clin Invest* 2011; 121: 3804-3809.
- [55] Wilcken N, Zdenkowski N, White M, Snyder R, Pittman K, Mainwaring P, Green M, Francis P, De Boer R, Colosimo M, Chua S, Chirgwin J, Beith J and Bell R. Systemic treatment of HER2-positive metastatic breast cancer: a systematic review. *Asia Pac J Clin Oncol* 2014; 10 Suppl S4: 1-14.
- [56] Shi Z, Yang WM, Chen LP, Yang DH, Zhou Q, Zhu J, Chen JJ, Huang RC, Chen ZS and Huang RP. Enhanced chemosensitization in multi-drug-resistant human breast cancer cells by inhibition of IL-6 and IL-8 production. *Breast Cancer Res Treat* 2012; 135: 737-747.
- [57] Xia L, Tan S, Zhou Y, Lin J, Wang H, Oyang L, Tian Y, Liu L, Su M, Wang H, Cao D and Liao Q. Role of the NF κ B-signaling pathway in cancer. *Onco Targets Ther* 2018; 11: 2063-2073.
- [58] Yeh WL, Tsai CF and Chen DR. Peri-foci adipose-derived stem cells promote chemoresistance in breast cancer. *Stem Cell Res Ther* 2017; 8: 177.
- [59] Chen DR, Lu DY, Lin HY and Yeh WL. Mesenchymal stem cell-induced doxorubicin resistance in triple negative breast cancer. *BioMed Res Int* 2014; 2014: 532161.
- [60] Chu QD, Panu L, Holm NT, Li BD, Johnson LW and Zhang S. High chemokine receptor CXCR4 level in triple negative breast cancer specimens predicts poor clinical outcome. *J Surg Res* 2010; 159: 689-695.
- [61] Xue G, Restuccia DF, Lan Q, Hynx D, Dirnhofer S, Hess D, Rüegg C and Hemmings BA. Akt/PKB-mediated phosphorylation of twist1 promotes tumor metastasis via mediating cross-talk between PI3K/Akt and TGF- β signaling axes. *Cancer Discov* 2012; 2: 248-259.
- [62] Landry BD, Leete T, Richards R, Cruz-Gordillo P, Schwartz HR, Honeywell ME, Ren G, Schwartz AD, Peyton SR and Lee MJ. Tumor-stroma interactions differentially alter drug sensitivity based on the origin of stromal cells. *Mol Syst Biol* 2018; 14: e8322.
- [63] McMillin DW, Delmore J, Weisberg E, Negri JM, Geer DC, Klippel S, Mitsiades N, Schlossman RL, Munshi NC, Kung AL, Griffin JD, Richardson PG, Anderson KC and Mitsiades CS. Tumor cell-specific bioluminescence platform to identify stroma-induced changes to anticancer drug activity. *Nat Med* 2010; 16: 483-489.
- [64] Straussman R, Morikawa T, Shee K, Barzily-Rokni M, Qian ZR, Du J, Davis A, Mongare MM, Gould J, Frederick DT, Cooper ZA, Chapman PB, Solit DB, Ribas A, Lo RS, Flaherty KT, Ogino S, Wargo JA and Golub TR. Tumour micro-environment elicits innate resistance to RAF inhibitors through HGF secretion. *Nature* 2012; 487: 500-504.
- [65] Ni Y, Zhou X, Yang J, Shi H, Li H, Zhao X and Ma X. The role of tumor-stroma interactions in drug resistance within tumor microenvironment. *Front Cell Dev Biol* 2021; 9: 637675.
- [66] Marusyk A, Tabassum DP, Janiszewska M, Place AE, Trinh A, Rozhok AI, Pyne S, Guerriero JL, Shu S, Ekram M, Ishkin A, Cahill DP, Nikolsky Y, Chan TA, Rimawi MF, Hilsenbeck S, Schiff R, Osborne KC, Letai A and Polyak K. Spatial proximity to fibroblasts impacts molecular features and therapeutic sensitivity of breast cancer cells influencing clinical outcomes. *Cancer Res* 2016; 76: 6495-6506.